Eur. Phys. J. D **34**, 263–269 (2005)
DOI: 10.1140/epjd/e2005-00108-7

THE EUROPEAN PHYSICAL JOURNAL D

Silver nanowires

A. Graff[1], D. Wagner[2], H. Ditlbacher[3], and U. Kreibig[2,a]

[1] Institut für Festkörper- und Werkstoffforschung, 01171 Dresden, Germany
[2] I. Physikalisches Institut A, RWTH, Aachen, Germany
[3] Karl-Franzens-Universität, Graz, Austria

Received 6 September 2004
Published online 13 July 2005 –

Abstract. Free silver nanowires were produced in aqueous electrolyte by a novel chemical reaction. Their diameters are about 27 nm, the lengths range up to more than 70 μm, yielding extreme length to thickness-ratios up to 2500. Their structure was identified by TEM analysis (SAED) and HRTEM to consist of a lattice aligned bundle of five monocrystalline rods of triangular cross-section forming an almost regular pentagonal cross-section. It is demonstrated that, for application purposes, single *free* nanowires can be mounted between contact areas. This manipulation is enabled by observing the nanowires in real time at atmosphere by Zsigmondy-Siedentopf farfield darkfield microscopy. Experimental results are presented concerning electrical dc–conductivity and optical plasmon polariton excitation, the latter obtained from a single *free* wire without substrate and a single wire deposited on quartz glass. We also report about a present research cooperation with the Graz group of Aussenegg and Krenn which is devoted to investigate plasmon propagation in our Ag nanowires and to prove application possibilities as information guide fibers – in analogy to optical fibers – which may be integrated into micro- and nanoelectronic circuits.

PACS. 68.65.-k Low-dimensional, mesoscopic, and nanoscale systems: structure and nonelectronic properties – 73.21.-b Electron states and collective excitations in multilayers, quantum wells, mesoscopic, and nanoscale systems – 73.63.-b Electronic transport in nanoscale materials and structures – 78.67.-n Optical properties of low-dimensional, mesoscopic, and nanoscale materials and structures

1 Silver nanowires

At present, nanowires find increased attention, probably due to general interest in size quantized electrical conduction, the enormous success of carbon nanotubes, and also due to the need of nanoelectronics for small connecting wires (for Ag [1–4,7–9]). Interesting for future applications may be plasmon-conducting fibers [2].

In this paper we report about nanowires of silver, which were created recently [1]. These wires, their atomic structures and some physical properties and possible applications will be described in the following.

Our own activities go back to 1971 [5] where *gold* rods up to length to thickness-ratios of $\leq 10^2$ were created chemically, applying a modified Zsigmondy method [6]. In Figure 1 (from 1971) we show a collection of different *gold* nanostructures, to demonstrate the variety of real quasi-equilibrium structures of the fcc lattice on the nanometer scale ranging from platelets and rods to almost perfect 5 and 20 tetrahedra twins. These shapes are created by prevalent growth directions. One of the icosahedral particles consisting of 5 tetrahedra is shown in the inset of Figure 1.

Nanowires and nanorods are nowadays produced from various metallic and semiconductor materials and with different methods (e.g. [1–4,7–9]) among which the chemical ones often yield perfect crystalline structures. Without doubt, most spectacular are at present compact and hollow carbon nanotubes. Shorter and more compact silver rods were recently analyzed by Hofmeister et al. [8].

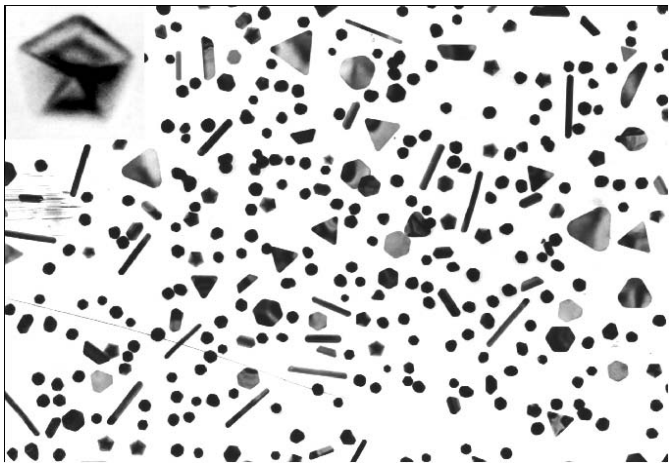

Fig. 1. Various gold nanostructures, produced by the Zsigmondy aqueous colloid method [6]. Mean nanoparticle diameter 36 nm; longest nanowires 200 nm. Inset: 40 nm pentagonal twin gold nanoparticle [5].

[a] e-mail: kreibig@physik.rwth-aachen.de

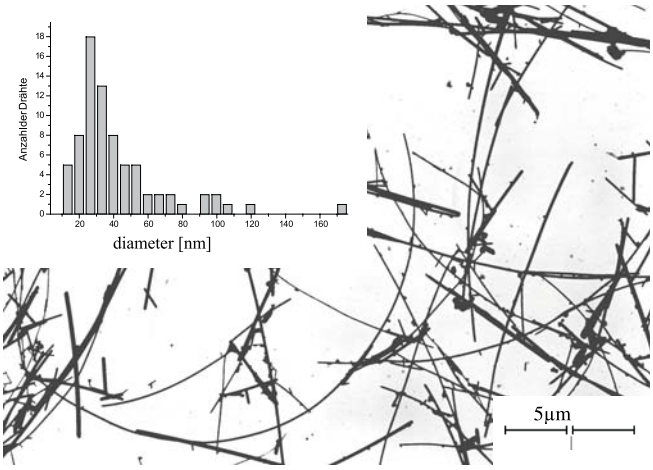

Fig. 2. Silver nanowires. Inset: diameter distribution.

The silver wires of the present investigation were produced by a novel chemical reduction method of Ag-ions in an aqueous electrolyte solution which yields, both, nanoparticles and nanowires.

Chemical details of this method will be given in a forthcoming paper, since a patent is pending. It should be pointed out already here that this chemical procedure does without any stabilization additive, in contrast to many other chemical production lines of nanorods and nanowires. After additional cleaning by dialysis, the wire surface is assumed to be contaminated by less problematic ions and molecule groups, only.

The purified wires were carefully separated from the also present nanoparticles and could be manipulated freely in the electrolyte while inspected by Zsigmondy darkfield farfield microscopy in real time.

2 Structural properties of the nanowires

Figure 2 shows a bright-field TEM micrograph of an example of the nanowire material [1] deposited on carbon foil. Figure 3 shows, in comparison, some wires in optical darkfield and in SEM microscopy. Since the former is due to the diffraction of elastically scattered light, the thickness appears drastically enlarged and so, only the wire lengths can be determined optically. The advantage of the darkfield microscopy is that observation and direct manipulation can be done simultaneously at air.

As obvious from Figure 2, wires with extremely large length-to-thickness ratios (up to 2500) are obtained with thicknesses from a well defined lower limit of 13 nm upwards. The thickness of the wires is usually constant along the whole length (with the exception of few exemplars where the thickness changes, preferentially, in steps). The end tips are either rounded or of asymmetric prismatic shape in the projection of the TEM image.

The largest thicknesses observed are below 150 nm. Remarkably, thicknesses exhibit a narrow unimodal probability distribution (Fig. 2, inset) close to log normal with a clear maximum at 27 nm and a halfwidth of

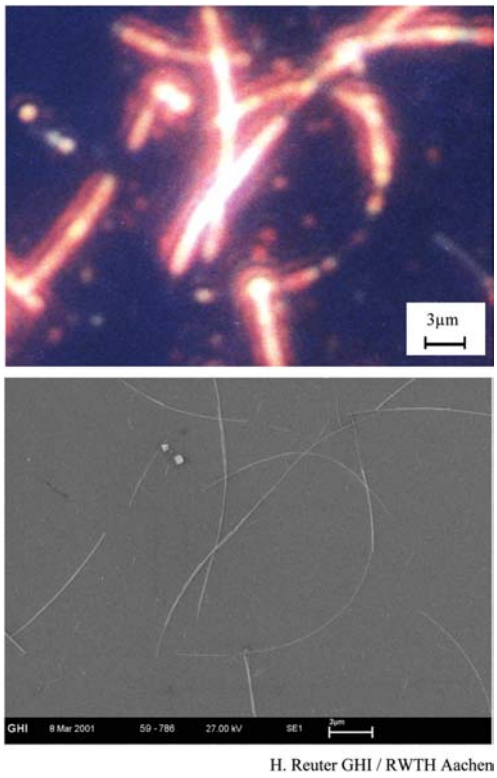

Fig. 3. Silver nanowires. Comparison of optical darkfield below the Abbe limit and scanning electron microscopy.

about ±10 nm. This proved to be characteristic for most of the production runs which we performed, hence it appears to be due to general structural stability limits. In contrast, no defined distribution is observed for the nanowire lengths, variable for more than a factor of 10^2 and up to 90 μm.

Due to increasing stability problems, we did not yet search for the ultimate wire sizes to be produced. The wires are stable at air when kept cool in the dark, up to several days. They are not stable if irradiated severely and for extended times by electrons in the TEM. At air, chemical reactions (e.g. by atmospheric sulfur compounds) take place and such reactions are accelerated by irradiation with light. Then, the wires break into small pieces, spontaneously or under weak external mechanical stress.

Two, possibly connected, effects may induce the wire growth: a pentagonal twin particle as nucleus (the size of which determining the observed minimum wire thickness), selective growth of the end tip planes, extremely enhanced by catalizing ingredients of the electrolyte, and, at same time, inhibition of growth in other directions by electrolyte ions and by electrostatic fields and double layers at the rod surfaces. Hence, the nanowires may be regarded as *nanowhiskers*.

The size distribution of the nanoparticles, created simultaneously, roughly starts at the thickness of the thinnest wires and most of them have sizes of the 2- to 3-fold of this thickness. With increasing thickness the average eccentricity of the particles increase, and there is a continuous transition in shape towards the rod and the

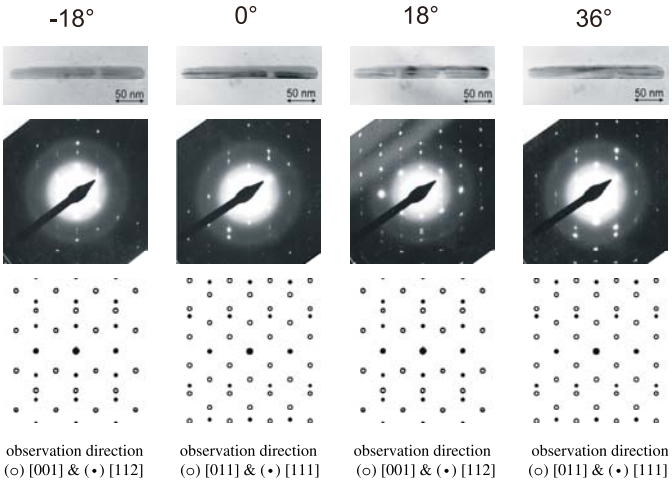

Fig. 4. Selected Area Electron Diffraction (SAED) of a silver nanowire rotated along its axis. The patterns are repeated after 36° rotation.

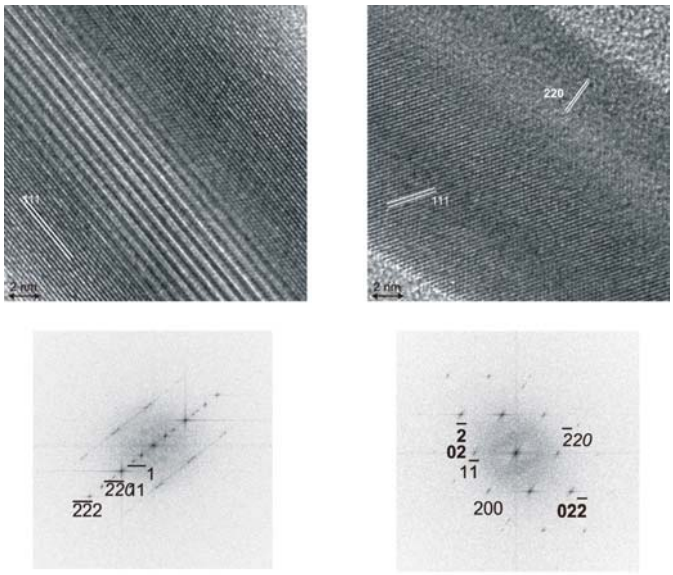

nanowire geometry. Few existing very thick wires and wires with varying thickness are obviously created by aligned side-by-side agglomeration of thin wires and subsequent lattice matched coalescence.

3 Analysis of the nanowires by HRTEM and SAED

Dark field TEM and HRTEM micrographs and SAED patterns of *single* wires give defined spots (Figs. 4 and 5), clearly indicating a well developed crystalline structure. Contrasts of crystal defects perpendicular to the wire axis were not observed. Results of the diffraction analysis are:

(1) the wires have the fcc-lattice structure of silver. One single crystal of silver with fcc structure can, however, not produce all the spots visible in the electron diffraction pattern of a *single* wire. By combining diffraction diagrams of silver with different zone axes the measured diffraction pattern could be simulated numerically;
(2) the long wire axis is in the (110) direction and perpendicular to the (220) lattice planes. The lattice planes parallel to the surface are either (220) or (111);
(3) the phase contrast in the bright areas forms stripes parallel to the wire axis pointing to prism shaped segments where the thickness changes perpendicular to the wire axis and is almost constant along the wire.

One possible explanation is a *five fold symmetry* round the wire axis as proposed recently for copper rods [7], for silver wires [2,4] and rods [8], and observed earlier [5] from gold nanoparticles as shown in Figure 1 which consist of five tetrahedra including a small misfit angle between them. The wires then consist of five almost identical rod-like segments which can be constructed from the cubic fcc structure of silver. Highest rotational symmetry is obtained when all segments have equal size.

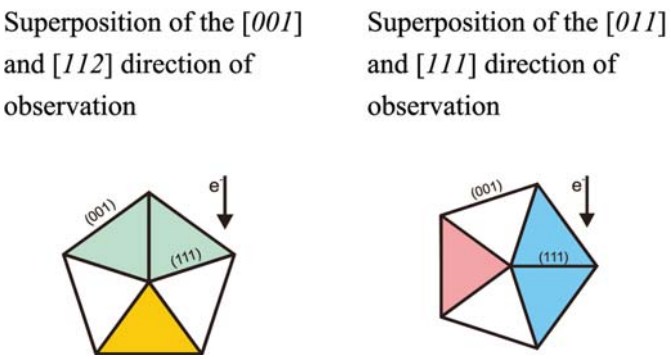

Fig. 5. High Resolution Transmission Electron Microscope (HRTEM) images and SAED patterns of a silver nanowire; left: symmetrical orientation against the electron beam, right: asymmetrical orientation against the electron beam.

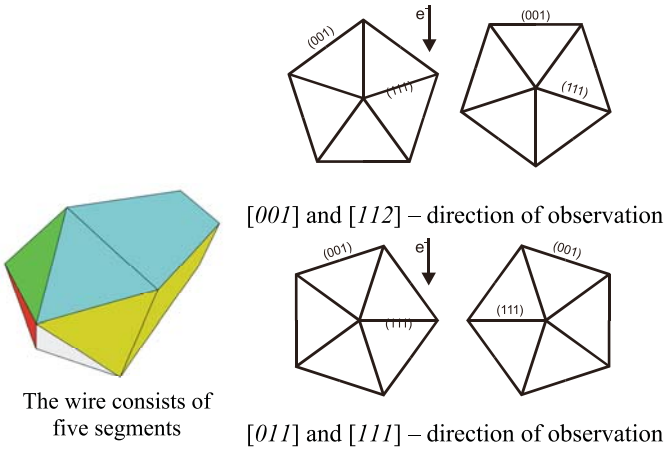

Fig. 6. Model of the silver nanowire structure [7] with identical segments.

Putting five of these segments together, with the (001) surfaces to the outside, a compact, well crystallized wire is formed (Fig. 6). The cross-sectional shape of the

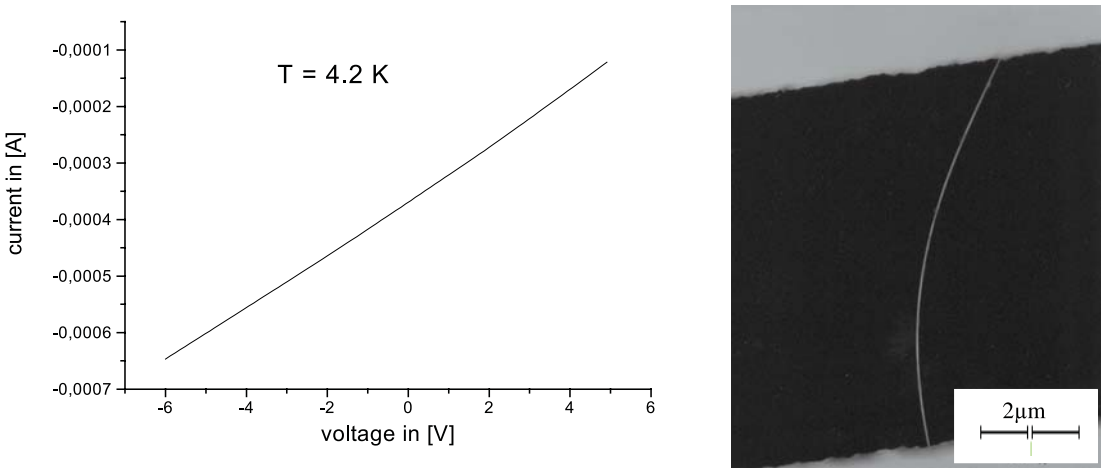

Fig. 7. Left: DC current/voltage characteristic of a single free silver nanowire mounted between two Ag/Cu-contacts. Diameter $D = 50$ nm. Right: TEM image of the same free wire between the contacts.

wire is pentagonal, consisting of a bundle of five identical fibers of triangular cross-section connected by coherent twin boundaries. Regarding the plane defined by the wire axis and the incident electron beam, two different zone axis orientations were identified by rotating the wire around its axis for 18°. This is shown in Figure 4 and modelled in Figure 6. Figure 5 shows HRTEM images for the indicated symmetric and asymmetric orientation, respectively, together with the diffraction plots.

From further diffraction experiments rotating the samples follows that the angle between the two long (111) surfaces of the segments (i.e. at the wire axis) is 70.53°. This value differs from 72° necessary to fill completely the wire with five of these segments. We have a misfit angle similar to the pentagonal nanoparticles of Figure 1 [5]. Like for the mentioned gold particles, it appears surprising why nature takes that strange way to form stable fcc-structured nanowires.

One possible way to form a densely packed structure is the introduction of small angle grain boundaries were two (111) surfaces of two segments touch each other. Due to the small diameter of the wires additional lattice planes have not to be introduced. A small deformation of the segments shifting the center of the axis should be sufficient to form a pentagonal cross-section taking the misfit angle into regard. Alternatively, the misfit region might either be closed by elastic strain, or by filling with disordered atoms. By the way, this minute angle misfit may cause the narrow thickness distribution and be the reason why many of the wires exhibit characteristic curvatures as obvious in Figure 2.

4 DC–conductivity

In the few nanometer region, electrical conductivity does no longer follows the Ohm mechanism of incoherent scattering of conduction electrons by lattice imperfections, but is dominated by coherent, surface boundary determined modes of the macroscopic all-electron wavefunctions, sometimes also modelled as *ballistic* conductivity. Relevant quantity for the formation of modes is λ_e/D with electron wavelength λ_e and wire diameter D which, in our case, is too small to expect the formation of modes with low quantum numbers even if we assume that the diameter of the single triangular filament is the relevant size. However, due to the excellent quality of, both, crystalline structure and surface properties, special higher modes might be effective at very low temperatures. Hence, we performed measurements of the dc-conductivity of our Ag nanowires applying a Keithley 2400 Source Meter equipment of high sensitivity. Lowest available temperature was, up to now, 4.2 K but experiments are now extended to 1.5 K. We measured at a single *free* nanowire immersed in the liquid He bath which was mounted between two electric contact areas. E.g., from carbon nanowires it is known that electrical contacts of unsatisfying quality are a major problem. Hence, a special technique was developed to reduce the contact resistances. A patent is pending. Since TEM characterization was required to obtain thickness data of the measured wire, the sample preparation was quite complex and laborious.

The obvious linearity of the I/U characteristic in Figure 7 confirms the validity of Ohm's law for our nanowires. Careful inspection shows, however, a slight increase of conductivity towards higher voltage, a small effect which we do not yet understand. The planned experiment to further reduce the temperature for a factor of about 3 may be helpful.

The numerical evaluation of our low temperature experiments gave for a 50 nm diameter free silver wire the resulting resistivity of $\rho_{\mathrm{wire}} = 1.63 \times 10^{-6}\ \Omega\,\mathrm{m}$ at 4.2 K.

This value includes electron scattering at surfaces and lattice defects and the contact resistance in unknown proportions. This renders a detailed comparison with bulk silver difficult.

In nanostructures with dimensions clearly smaller than the electron mean free path in the bulk, the dominant conduction electron scattering effect is usually the diffuse surface scattering [9]. According electron mean free paths are

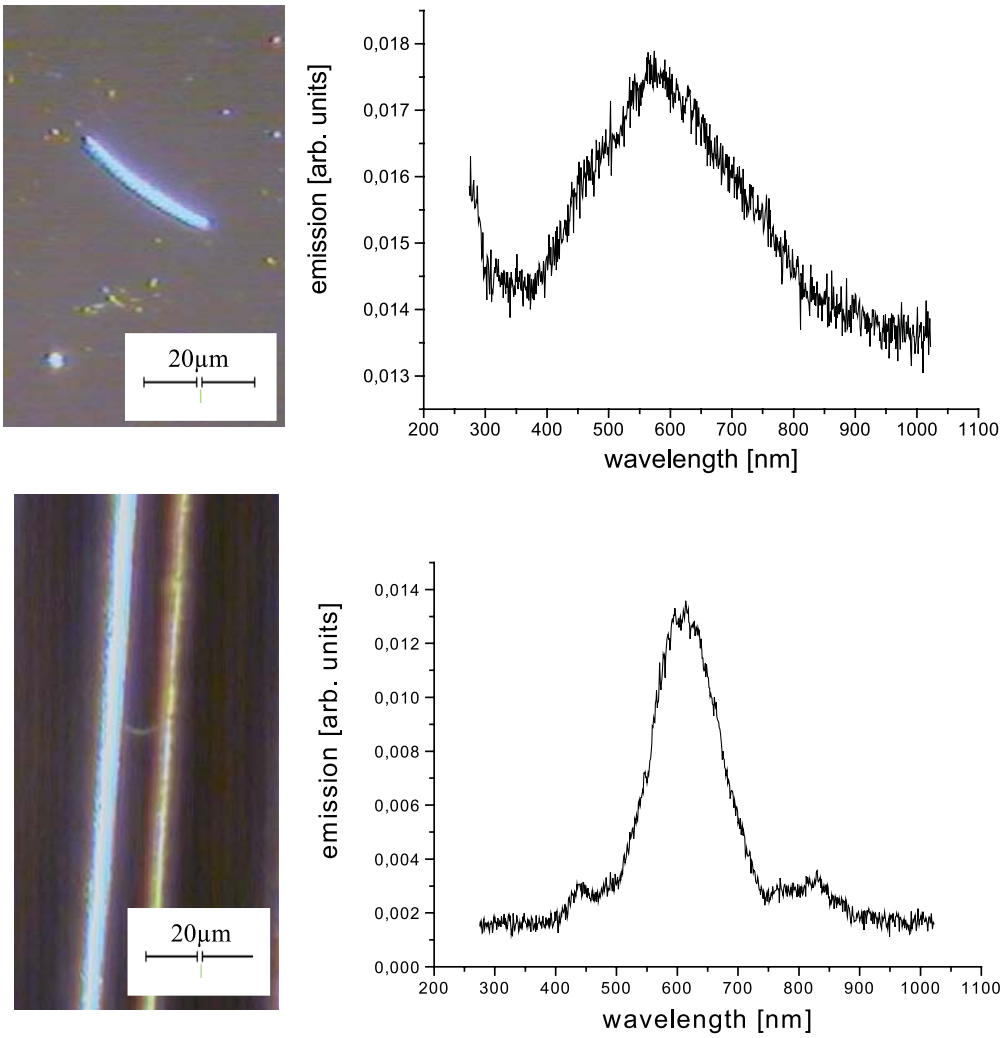

Fig. 8. Optical spectra of the darkfield emission of single silver nanowires deposited on a quartz glass substrate (upper figures) and mounted freely between two carrier plates (lower figures); left: optical darkfield images, right: emission spectra.

at present being calculated [10]. Estimated very roughly, in our case it equals about the double wire diameter if diffuse surface scattering is assumed. However, the wires are well crystalline and their surfaces are almost atomically flat, suggesting that the *Fuchs* specularity factor may be large. Problems also arise from the fivefold symmetry and the inner coherent grainboundaries. In the course of the theoretical evaluation, done at present, we hope to gain information about the quality of the contacts, too.

5 Optical plasmon polariton excitation

The all-conduction-electron wavefunction can be inspected, as well, at high frequencies by making use of the optical excitation of plasmon polaritons. In the nanowire, special polariton modes are expected. Since the wire lengths usually exceed the light wavelengths by far, quasistatic conditions [6] never hold. The modes are, due to the anisometry of the specimen, drastically polarization dependent: there are resonance modes in the optical frequency region if the electric vector of the incident light is normal to the silver wire axis, while the resonance frequency for the parallel polarization modes shift towards zero frequency with increasing wire length [12]. At finite lengths the modes are influenced by the boundary conditions close to both end tips. To our knowledge, no general calculation of these modes exists, however, from the model of elongated ellipsoids some qualitative informations as those given above, can be drawn [6].

By combining the optical Zsigmondy-Siedentopf farfield darkfield observation method with a diode array spectrophotometer Zeiss MCS, we were able to record the plasmon polariton emission spectrum (i.e. elastic light scattering spectrum) of a *single* Ag nanowire deposited on a quartz glass substrate. Quite recently we even succeeded to measure the light emission of a *single, free* Ag-nanowire without any substrate.

Results of both experiments are shown in Figure 8. The irradiation beam diameter was chosen larger than the wire length, but the detector beam diameter was chosen to be much smaller.

In spite of the problems with linear polarization arising from convergence and reflections of the light beam in the darkfield equipment, we were, in our most recent experiments, able to clearly separate the polarization dependent spectra. This will be the topic of a subsequent paper.

The observed, unpolarized spectra of Figure 8 exhibit a well pronounced maximum at about 600 nm in both experiments due to the electrical field components normal to the wire axis. (It may be mentioned that we earlier [12] measured 2 nm silver nanoparticles to have their Mie resonance at about 380 nm when deposited on quartz glass and at 340 nm when being in a *free* cluster beam.) The broad wings of the bands point to the superposition of different polariton modes which are expected to be excited simultaneously in long wires.

The most striking change between the deposited and the free nanowire is the large difference in emission band width. While we observed a moderate width of roughly 0.7 eV in the former case, the width is drastically reduced to only o.35 eV, when the wire is *free*. This indicates the strong, non-classical Ag/oxide-substrate interaction which we earlier observed from Ag-nanoparticles with and without oxide substrates (e.g. [12]). In these nanoparticle experiments we found widths of 0.6 eV (with quartz glass support) and 0.25 eV (in the free beam), respectively. Hence, the influences of quartz substrate are of similarly large magnitude for Ag nanoparticles and nanowires.

6 Plasmon polariton transport in nanowires

In the former section, experiments were described where the diameter of the incident light beam exceeded the length of the nanowire. Hence, modes were excited in the whole specimen. (However, the detector beam width was much smaller.)

If, in contrast, the excitation region is concentrated at one of the end tips, locally excited plasmon modes can propagate through the wire and can be used to carry information from one end tip to the other end tip. This system resembles usual light guide fibers with two principal differences:

(a) modes not of the light field but of the electron wave functions propagate. The wavelengths of the conduction electrons in silver being shorter for a factor of about 10^4 than of light, the according fiber thickness can be smaller for orders of magnitude.
The fundamental difference is that modes in optical fibers are standing wave configurations ("geometrical" or "morphological" resonances) where $\lambda_{\text{optical}}/D$ determines the quantum number and is <1, while plasmon polaritons are material resonances determined essentially by the optical dielectric function where D can be $\ll\lambda_{\text{optical}}$ and no defined cut-off size exists as for the morphological resonances in the optical wave guides;
(b) light guides consist of transparent dielectrics, ensuring extremely long propagation lengths of optical modes, while the plasmon polariton life times in metallic nanowires are extremely short, amounting to some 10 fs at most [12]. Hence, the propagation lengths L_{plasmon} of localized plasmon polariton modes are expected to be short;
(c) if we extrapolate our knowledge about plasmon polaritons in spherical nanoparticles, we can predict that damping increases with decreasing wire diameter due to electron-surface interactions and hence, transport lengths will additionally decrease.

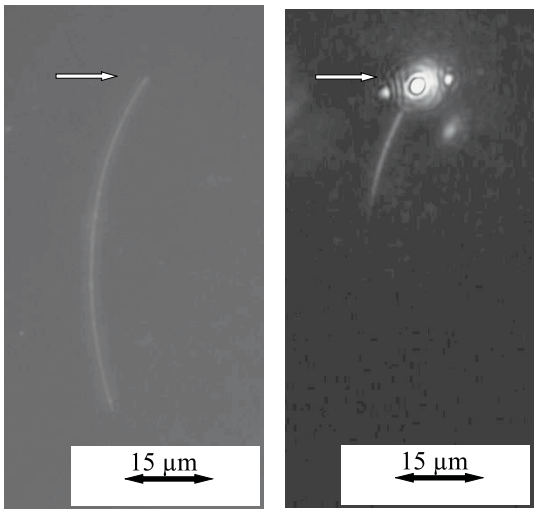

Fig. 9. Propagation of locally excited plasmons in a silver nanowire embedded in a fluorescing matrix [2]. Left: optical darkfield image (thickness 25 nm; length 50 μm). Right: laser irradiation spot at top. Fluorescence emission along the wire for, rougly 15 μm.

Application of *plasmon polariton information transport*, thus is limited to short but not too thin wires and will be restricted, e.g., to single microelectronic building units.

In a cooperation with the group of Aussenegg, Krenn and Ditlbacher of the Karl-Franzens-Universität of Graz [14], realistic limitations of L_{plasmon} in our wires are going to be measured to control the influence of the plasmon lifetimes. Since, among all metals, silver has the most pronounced plasmon modes and long plasmon phase lifetimes, our silver nanowires appear to be well suited for such experiments which are performed at present. Figure 9 demonstrates first experimental results of Ditlbacher [2] obtained from a roughly 25 nm thick and 50 μm long Ag nanowire (optical darkfield image Fig. 9, left) which was deposited onto a quartz slab and surrounded by a 30 nm PMMA-layer doped with fluorescing agent (DiR) which acts as transformer from the electromagnetic near field close to the interface into farfield radiation. The details of the optical properties and of the experiment are given in [2]. The wire was irradiated by a 785 nm laser beam focused onto the upper end tip. By the fluorescence farfield radiation the propagation of the plasmon polariton is clearly visible along a propagation path length of more than 10 μm (Fig. 9 right). To our knowledge, this is the first observation of plasmon polariton propagation in nanowires.

References

1. D. Wagner, A. Graff, U. Kreibig, *Structure and Properties of Silver Nanowires*, Proceedings B XIII-6, ISSPIC 11, Strasbourg, France, 2002
2. H. Ditlbacher, thesis, Karl-Franzens-Universität Graz, 2003
3. J.Q. Hu, Q. Chen, Z.-X. Xie, G.-B. Han, R.-H. Wang, B. Ren, Y. Zhang, Z.-L. Yang, Z.-Q. Tian, Adv. Funct. Mat. **14**, 183 (2004)
4. S. Nepijko, D. Ievlev, W. Schulze, J. Urban, G. Ertl, ChEMPHYSCHEM 2000, p. 140
5. U. Kreibig, thesis, Universität des Saarlandes, 1971; U. Kreibig, Nanostructured Metal Clusters and Colloids, in *Handbook of Surfaces and Interfaces of Materials*, edited by H.S. Nalwa (Academic Press, San Diego, 2001), Vol. 3
6. U. Kreibig, M. Vollmer, *Optical Properties of Metal Clusters* (Springer Series in Materials Science, 1995)
7. I. Lisiecki, A. Filankembo, H. Sack-Kongehl, K. Weiss, M.P. Pileni, J. Urban, Phys. Rev. B **61**, 4968 (2000)
8. H. Hofmeister, S. Nepijko, D, Ievlev, W. Schulze, G. Ertl, J. Crystal Growth **234**, 773 (2002)
9. R. Hillebrand, H. Hofmeister, K. Scheerschmidt, J. Heydenreich, Ultramicroscopy **49**, 252 (1993)
10. S. Ino, J. Phys. Soc. Jap. **21**, 346 (1966); T. Komoda, Jap. J. Appl. Phys. **7**, 27 (1968)
11. J. Abels, private communication
12. U. Kreibig, M. Quinten, A. Hilger, Optical Materials/ Heterogeneous Materials, in *Encyclopedia of Modern Optics*, edited by B. Guenther, L. Bayvel, D. Steel (Elsevier, London, 2003)
13. M. Quinten, private communication
14. First plannings at *ESF-PESC Exploratory Workshop on Surface-Plasmon Photonics*, Obernai, France, April 2001